Simulation of Deuteron Tails Produced by Close Collisions with ICRH Accelerated He³ Ions in JET

F.S. Zaitsev[1,a], A. Gondhalekar[2], T.J. Johnson[3],
S.E. Sharapov[2], D.S. Testa[4], I.I. Kurbet[1] and JET EFDA contributors[*]

[1]*Moscow State University, Faculty of Computational Mathematics and Cybernetics, RF*
[2]*EURATOM/UKAEA Fusion Association, Culham Science Centre, Abingdon, UK*
[3]*Association EURATOM-VR, Alfven Laboratory, Royal Institute of Technology,*
10044 Stockholm, Sweden
[4]*CRPP, Association EURATOM - Confederation Suisse, EPFL, Lausanne, Switzerland*
[a]*e-mail: zaitsev@cs.msu.su*

1. Introduction. Collisions between charged particles in a plasma are usually considered as Coulomb collisions with small fractional energy exchange and small scattering angles. However, high-energy particles can participate in close collisions with a large energy exchange when the minimum distance of approach between particles is such that the strong nuclear force comes into play. Theoretical and experimental studies of this effect showed that Nuclear Elastic Scattering (NES) of energetic α-particles with thermal ions forms MeV energy range deuterium and tritium tails, which can give a significant contribution to the α-particle signal on a Neutral Particle Analyser (NPA) [1,2].

Experimental data on the NES knock-on deuterium was later collected on JET for discharges with ICRF-heating of He³ minority, where close collisions between fast He³ ions and thermal deuterons produced a deuterium tail. Interpretation and planning of such experiments and understanding the underlying processes require accurate modelling of both He³ and deuterium. The complexity of the problem is determined by the strong anisotropy of ions in velocity and spacial coordinates and the necessity to solve 3D kinetic problems accounting for the large orbit widths, friction and diffusion in velocity, neo-classical radial transport, pitch angle scattering, NES, etc.

2. Formulation of the problem. The model is based on the results of Refs. [3,4]. The 3D trajectory-averaged kinetic equation for the deuterium distribution function f_d^0, using a full 3D collisional operator and allowing for NES with He³, has the form

$$\frac{\partial f_d^0}{\partial t} = \frac{v_c^3}{\tau_c} \sum_{n=1,4,5} \frac{1}{\langle 1 \rangle} \frac{\partial}{\partial \bar{x}^n} \left[\sum_{m=1,4,5} \left(A_{nm} \frac{\partial f_d^0}{\partial \bar{x}^m} \right) + B_n f_d^0 \right] + \bar{S}_d - \frac{f_d^0}{\tau_{d,loss}}. \qquad (1)$$

The equation is drift trajectory averaged, with friction and diffusion over velocity, neo-classical radial transport, pitch-angle scattering, etc. The trajectory averaged neo-classical collisional operator and notation from Ref. [4] has been used (more details can be found in [5]). For the simulations here, Coulomb collisions with the Maxwellian deuterium and electrons are taken into account. Self-collisions at high energies and collisions with He³ are neglected, due to the small densities of the appropriate particles. The term $\bar{S}_d$ is the trajectory averaged NES source strength in constants of motion space $(\bar{x}^1, \bar{x}^4, \bar{x}^5) \equiv (\gamma_0, v_0, \theta_0)$, $\bar{S}_d(t, \gamma_0, v_0, \theta_0) = \langle S_d \rangle / \langle 1 \rangle$, where $S_d = S_d(t, \gamma(\gamma_0, \xi, v_0, \theta_0), \xi, v(\gamma_0, \xi, v_0, \theta_0), \theta(\gamma_0, \xi, v_0, \theta_0))$ is the local NES source strength per unit 6D phase space, γ is the half-width of the poloidal magnetic flux surface in the equatorial plane, ξ is the poloidal angle, v is the velocity, θ is the pitch-angle, $\gamma_0 \equiv \bar{x}^1$ is the half-width of the magnetic flux surface at the reflection point for trapped particles or at the innermost

---

point of the trajectory for passing particles, $v_0 \equiv \bar{x}^4$ is the generalised speed appropriate to the sum of kinetic and potential energies, $\theta_0 \equiv \bar{x}^5$ is the pitch-angle at the outermost point of the trajectory, $\langle 1 \rangle$ is the trajectory averaged Jacobian representing the transformation from Cartesian to the constants of motion coordinates $\bar{x}^n$.

The original form of the NES source S_d (Ref. [3], Eq. (11)) can be rewritten in a form much more suitable for numerical calculations and clarity

$$S_d(t, \gamma, \xi, v, \theta) = \frac{8\gamma_d^2 n_d(t, \gamma)}{v} \int_{\gamma_d v}^{+\infty} \frac{d\sigma(v_\alpha)}{d\Omega} v_\alpha dv_\alpha \int_0^\pi f_\alpha(t, \gamma, \xi, v_\alpha, \theta_\alpha(\chi)) du \qquad (2)$$

with the subscript α denoting He^3, $\theta_\alpha(\chi(v, v_\alpha, \theta, u)) = \arccos(\cos\psi\cos\theta - \cos u \sin\psi\sin\theta)$, $\gamma_d = (m_d + m_\alpha)/(2m_\alpha)$, $\psi = 1/2(\pi - \tilde{\theta}(\gamma_d, v, v_\alpha)) \in [0, \pi/2]$, $\tilde{\theta} = 2\arcsin(\gamma_d v/v_\alpha) \in [0, \pi/2]$, $d\sigma/d\Omega$ is the differential cross section for NES of He^3 with a deuterium target.

The loss term in Eq. (1) models the direct losses of particles to the wall due to deviations of the trajectories from the flux surfaces. Ripple losses are taken to be negligible, as discussed in Ref. [1].

Extensive tests show that the kinetic equation should be solved numerically for the perturbation to close to Maxwellian deuterium distribution, which satisfies Eq. (1) with $S_d = 0$, rather than the full distribution, in order to generate results with acceptable accuracy. A zero initial perturbation to the deuterium distribution was therefore set. A zero boundary condition at $v_0 = v_{0,\min}$ and zero fluxes at all other boundaries were used.

3. Algorithms and software. The distribution of He^3 in the presence of an ICRF wave field is calculated with the Monte-Carlo code SELFO [6]. This is used as input to the Fokker-Planck code FPP-3D [2,5], which can treat the overwhelming majority of other known kinetic effects. FPP-3D produces the distribution of the knock-on deuterium taking account of NES and calculates He^3 and deuterium signals along the vertical line-of-sight of the NPA.

A production FPP-3D run takes about 1 hour for deuterium on a Pentium IV with 3 GHz, requires $\sim .5$ Gb RAM and .7 Gb disk space. Sufficient number of grid points is $N_v \sim 70$, $N_\theta \sim 70$, $N_\gamma \sim 15$, $N_\xi \sim 25$. However, due to the accurate numerical treatment of the problem [5], 1.5 times less points in each N already gives good approximation.

4. Simulation of Deuteron Tails. Plasma parameters appropriate to JET He^3 ICRH discharges 53807, 53809, 53810, 53811 were used at $t = 9.5$ s. The characteristic values are: the magnetic axis R_{mag} was ~ 3 m with a minor radius ~ 1 m and an elongation ~ 1.5. The toroidal field $B(R_{mag})$ was ~ 3.5 T, the plasma current was ~ 1.8 MA. The core temperature $T_d(0) \sim 2$ keV, $T_e(0) \sim 4.3$ keV and density $n_{d,e}(0) \sim 1.8 \times 10^{19}$ $1/m^3$. NPA measurements of He^3 were made in the first two discharges; those of deuterium in the last.

Analysis of the NES source S_d shows that one can expect the main effect to be a distortion of the deuterium distribution at energies 0.2 - 1 MeV at radii $\gamma \sim 0$ - 0.5 m.

In order to compare simulations with NPA measurements, the line integral distribution (LID) functions for deuterium (and He^3) were calculated

$$\bar{F}_d(t, E) = \sqrt{\frac{2E}{m_d^3}} \int_{Z_p^{(1)}}^{Z_p^{(2)}} f_d^0(t, \gamma_0(\gamma, \xi, v, \theta), v_0(\gamma, \xi, v, \theta), \theta_0(\gamma, \xi, v, \theta)) dZ, \qquad (3)$$

where $Z_p^{(k)}$, $k = 1, 2$ are points of the Cartesian coordinate Z at which the NPA chord intersects the plasma boundary; $\gamma = \gamma(Z)$, $\xi = \xi(Z)$, $\theta = \theta(Z)$ in (3) are functions of the coordinate along the NPA line of sight. The NPA chord in JET goes vertically

at major radius $R = 3.07$ m, which is close to the magnetic axis, and detects particles with pitch-angle $\theta \approx \pi/2$. Fig. 1 shows calculated and measured He^3 and deuterium LIDs. Fig. 1 (top) shows the NPA data which was collected for He^3 only in discharge 53807, versus He^3 data computed with SELFO code. Fig. 1 (bottom) shows on the other hand the NPA data which was collected for deuterium only in discharge 53810, versus deuterium knock-on tail calculated with FPP-3D code. It is seen how both the primary He^3 distribution function and the knock-on deuterium tail agree between the NPA data and the calculation

Steady-state in NES deuterium LID is established in less than 3 s. So in JET He^3 ICRH experiments on the scale of 10 s the maximum possible NES effect is reached. Moreover deuterium LID closely follows He^3 evolution. Calculations show that trajectory widths can not be ignored for the correct calculation of LIDs for energetic particles. SELFO runs with different number of particles allow one to conclude that local fluctuations in LIDs are caused by Monte-Carlo approximation of the He^3 distribution.
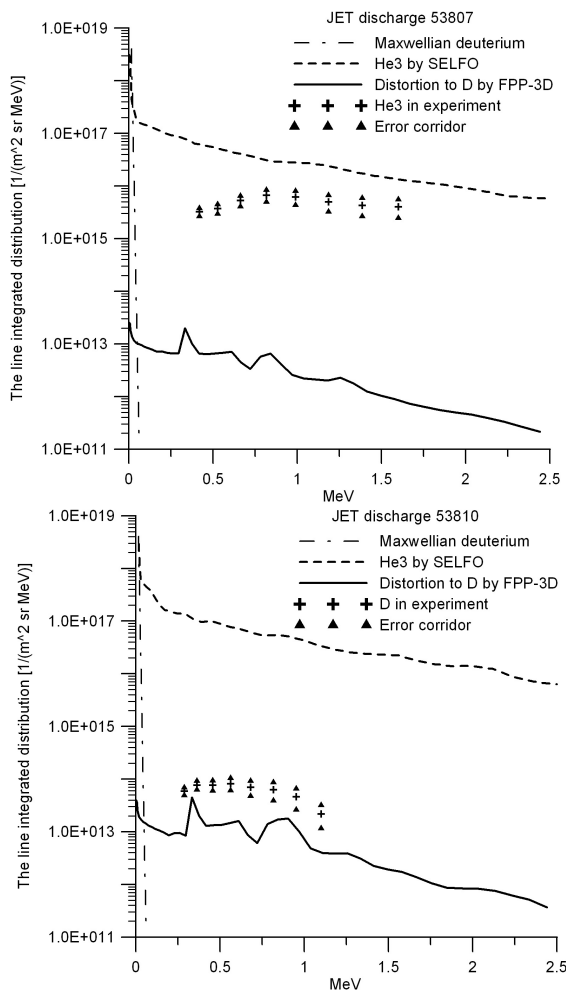

Figure 1: He^3 and D LIDs at $t = 9.5$ s. Crosses give measured data, upper and lower triangles - error range in a measurement. Dashed lines show SELFO calculations, solid - FPP-3D.

It is interesting to note, that a broad local structure near 0.5 MeV was also present in experimantal and calculated NPA spectra of α-particles and NES perturbed deuterium and tritium in JET DTE 1 experiments [2].

Figs. 2, 3 give He^3 and deuterium distributions over the energy and the distance along the NPA chord with zero distance appropriate to $Z_p^{(1)}$, the farthest from the NPA point on the plasma boundary, and the maximum distance to $Z_p^{(2)}$, the nearest. Plots 2, 3 allow one to understand which phase space regions contribute most to the NPA signal at a fixed energy. Local maximums are explained by the propagation of the NPA chord through areas of different NES source intensity, formed by the He^3 distribution, i.e. by He^3 ICRH. In the case of He^3 the flux surfaces with $\gamma \approx 0 - 0.5$ m give the most contribution at energies $\sim 200 - 500$ keV and $\gamma \approx 0.5$ m for higher energies. For deuterium one can see similar behaviour in pulse 53807. In pulse 53810 the central regions are more dominant for all energies due to the different distribution of ICRH He^3. Qualitatively, the distribution of deuterium and He^3 NPA signal along the chord are in some sense similar in spite of the integral dependence of the NES source (2) on He^3 and the influence of other terms in Eq. (1). An important conclusion is that for energies less than 700 keV the NPA signal is accumulated mostly at the central regions of plasma for both He^3 and deuterium. This means that with ICRH it is possible to measure plasma properties in places of maximum resonance, not just for He^3, but also for deuterium exploiting the NES effect.

5. Conclusion. In this paper we have shown the importance of the NES effect for the NPA measurements of energetic ions in JET pulses. It was found that the maximum possible magnitude of deuterium NES effect is achieved in JET He^3 ICRH experiments. The magnitude of the knock-on effect is somewhat lower than it was for α-particles in JET DTE 1 [2], but still very important for the correct interpretation of the NPA data.

An agreement between experiment and simulation is seen from the slope of the curves showing the tail temperature of both He^3 and knock-on deuterium.

Phase space regions which contribute to the NPA signal most were determined. Analysis of pulses with different ICRH localisation showed sensitivity of the deuterium distribution along the NPA chord to the He^3 anisotropy. The importance of the large orbit width effect for the NES perturbed deuterium distribution function was demonstrated.

Due to the magnitude of the charge exchange probability it can be less complicated to measure deuterium rather than He^3. Taking into account the localisation in phase space of the He^3 distribution, the dominance of local regions in the NPA signal and the known law for the He^3 spread in (2), one can try to solve the inverse problem for obtaining properties of the He^3 distribution using measurements of the NES deuterium.
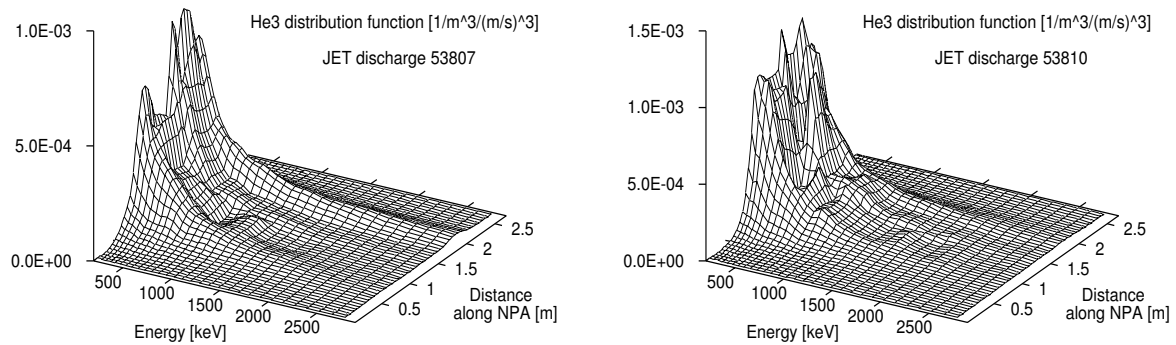

Figure 2: He^3 distribution over the energy and the distance along the NPA chord. FPP-3D calculation for SELFO He^3 distribution.
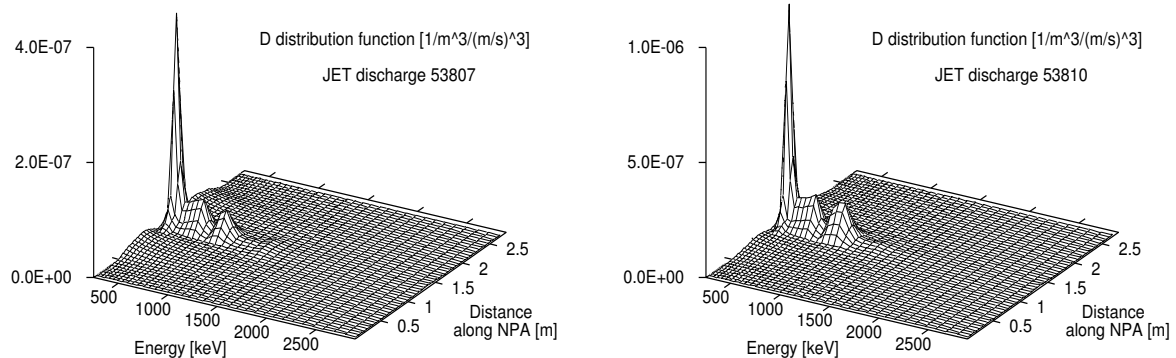

Figure 3: Deuterium distribution over the energy and the distance along the NPA chord. FPP-3D simulations.

References. [1] Korotkov A.A., Gondhalekar A., Akers R.J. Physics of Plasmas **7** (2000) 957. [2] F.S. Zaitsev, R.J. Akers, M.R. O'Brien. Nucl. Fusion **42** (2002) 1340. [3] Helander P., Lisak M., Ryutov D.D. Plasma Phys. Control. Fusion **35** (1993) 363. [4] Zaitsev F.S., O'Brien M.R., Cox. M.. Physics of Fluids B **5** (1993) 509. [5] F.S. Zaitsev. Mathematical modelling of toroidal plasma evolution. Moscow, MAX Press, 2005, 524 p. [6] Hedin J., Hellsten T., Eriksson L.-G., Johnson T. Nucl. Fusion **42** (2002) 527.